Available online at www.sciencedirect.com
SCIENCE DIRECT®
International Journal of Heat and Mass Transfer 49 (2006) 2304–2314
International Journal of HEAT and MASS TRANSFER
www.elsevier.com/locate/ijhmt

Multiple modes of a natural circulation evaporator

A. Baars *, A. Delgado

Technische Universität München, Lehrstuhl für Fluidmechanik und Prozessautomation, 85350 Freising, Germany

Received 27 May 2005; received in revised form 27 September 2005
Available online 23 February 2006

Abstract

The system behaviour of an open single tube, steam heated natural circulation evaporator has been investigated at heating steam pressures up to 0.44 MPa and different subcoolings of the process medium water. In the studied range of parameters, diverse operational states occurred which have been recognized for the first time as geysering coupled with manometer oscillation as well as first, second and third orders of density wave oscillation of type I. Due to the strong nonlinear behaviour of the system, up to three states appear in certain ranges of parameter constellations. By defined setting of initial conditions and distinct perturbations of the system, the individual states can be set.

Keywords: Natural circulation evaporator; Multiple modes; Geysering; Density wave oscillation

1. Introduction

The system behaviour of natural circulation evaporators has been presented in numerous literary works since this type of evaporator is widely used in different domains of industry, such as conventional/nuclear power plants [1,2], and chemical-, environmental-, food engineering and biotechnology [3–5]. This result of the simple and robust design due to the lack of moving elements. In the case of safety relevant systems like nuclear power plants, the application of natural circulation evaporators contributes to an improvement of passive safety [6]. Furthermore, in comparison to forced circulation systems, this type of evaporator enables a reduced mechanical exposure of shear and tensile stress to the process medium. This is especially important if liquid biomaterials are involved such as wort, a preliminary product of beer [7]. Besides these advantages, the operational behaviour of such systems has been recognized to be strong nonlinear [8]. This results from "the delicate balance between gravity head available due to downcomer and various pressure losses in the loop" [9].

In general, the desired operational state of a natural circulation evaporator is characterized by a stable two-phase flow [10] and fully developed boiling at the outlet of the heat exchanger. This mode appears only in limited constellations of process and geometry parameters. Outside of this limited range, different stationary and transient system behaviours emerge. Hereby, violent flow oscillations can cause intermittent and spatial thermal inhomogeneities in the process medium and can lead to the destruction of the apparatus. Bouré et al. [11] and Yadigaroglou [12] have described systematically different transient modes.

There is an interest in the start-up of natural circulation evaporators. Investigations revealed that on the path from high to low subcooling of the process mediums, a range of instabilities has to be passed [8]. A typical course of start-up modes consists of (a) a stable single-phase flow at high subcooling followed by (b) geysering/flashing and/or (c) type I density wave oscillations (DWO), (d) a stable two-phase flow at low subcooling [8,10,13–17]. Nearly all works reveal that the transient modes show almost constant frequencies and amplitudes at constant boundary conditions. By external pressurizing of the system using nitrogen for

* Corresponding author. Tel.: +49 8161 71 3275; fax: +49 8161 71 4510.
E-mail address: baars@wzw.tum.de (A. Baars).

0017-9310/$ - see front matter © 2006 Elsevier Ltd. All rights reserved.
doi:10.1016/j.ijheatmasstransfer.2005.10.046

Nomenclature

c_p	specific heat capacity, W/(kg K)
d	diameter overfall in the steam separator, m
g	gravitational acceleration, m/s^2
$\dot{m}$	mass flux, kg/m^2
$\dot{m}^*$	normalized mass flux ($=v_l/v_c$)
$\dot{m}^*_{Amp}$	normalized amplitude of mass flux ($=v_{l\,Amp}/v_c$)
n	order of density wave oscillation
p	heating steam pressure, MPa
r	enthalpy of evaporation, J/kg
t	time, s
v	flow velocity, m/s
v_c	characteristic velocity ($=\sqrt{g(H+d/4)}$), m/s
z	liquid level steam separator, m
z^*	normalized liquid level steam separator ($=z/d$)
z_{bb}	liquid filled length in the heated tube, m
A	cross sectional area, m^2
H	liquid charging level in feeding tank, m
L	length, m
N_{Bo}	boiling number ($=\frac{\dot{Q}}{A_H v_c \rho_f r}\frac{\rho_f-\rho_g}{\rho_g}$)
N_{Sub}	subcooling number ($=\frac{c_p \Delta\vartheta_{F\,Sub}}{r}\frac{\rho_f-\rho_g}{\rho_g}$)
$\dot{Q}$	heat flow, W
T	periodic time of oscillation, s
T^*	normalized periodic time ($=Tv_c/L_H$)

Greek symbols

λ	wave length of enthalpy oscillation, m
ϑ	temperature, °C
$\Delta\vartheta_{Sub}$	subcooling ($=\vartheta_b-\vartheta$), K
$\Delta\vartheta^*_{Sub}$	normalized subcooling ($=(\vartheta_b-\vartheta)/(\vartheta_b-\vartheta_F)$)
ρ	density, kg/m^3
τ	normalized time ($=tv_c/L_H$)
ζ	pressure drop coefficient

Subscripts

b	boiling
g	gas
i	index
l	liquid
E	exit of heated tube
F	feeding line to heated tube
FC	FFT coefficient
H	heated tube
HS	heating steam
I	inlet of heat exchanger
S	steam separator
U	isothermal manometer oscillation

Superscript

*	normalized value

inert gas, Jiang et al. [18] could maintain a stable single-phase mode over a certain range of subcooling during start-up. Hence, low quality DWO was suppressed. Besides the mentioned parameters of system pressure and subcooling, the concrete behaviour during start-up strongly depends on heat flux, geometry of the apparatus and the physical properties of the process medium.

In regard to the operational states mentioned above, geysering/flashing has been investigated systematically for the first time by Griffith [19] in closed vertical liquid filled lines. In the following, different types of geysering have been recognized in forced and natural circulation evaporators such as geysering coupled with manometer oscillations [20], geysering induced by condensation [15,16,21] or geysering similar to that occurring in closed vertical liquid filled lines [17]. Flashing has also been investigated by [14,16]. All works show the typical sequence: (1) incubation, (2) vapour generation and expulsion, (3) and refilling described by [12].

The phenomenon of density wave oscillation is well known in literature. A comprehensive description of this mode is given by [12]. Fukuda and Kobori [22] distinguish between oscillations with nearly zero steam quality (type I) and relatively high steam quality (type II) at the exit of the evaporator. Both modes feature an oscillating void fraction at the outlet of the heat exchanger. Due to the nearly zero steam quality/low void fraction, gravitational pressure drop governs the system in case of type I, while frictional pressure drop dominates type II. Yadigaroglu and Bergles [23] reported as the only ones on higher mode density wave oscillations which appeared at high subcoolings and low heat fluxes. They define the order of the oscillation as follows:

$$n = z_{bb}/\lambda. \tag{1}$$

The value z_{bb} represents the length of the single-phase region and λ the wavelength of the enthalpy oscillations in the single-phase region. The enthalpy oscillations result from the oscillating residence time of the individual liquid elements in the single-phase part of the heat exchanger. After passing the boiling boundary, they are transferred into void oscillations. For $\lambda > z_{bb}$ Yadigaroglu et al. call the mode "fundamental" or "zero order"; they observe a maximum order of six.

Due to the nonlinear behaviour of natural circulation evaporators, multiple operational states can appear at one parameter constellation. This has been shown theoretically by Knaani et al. [24], who explain this bifurcation

phenomenon with the non-monotonic behaviour of the buoyancy and friction forces, and the discontinuities due to transition between two-phase flow patterns. Experimental works indicate that multiple states arise especially at transitions of operational states. Yadigaroglu and Bergles [23] revealed at low subcoolings and low heat flux in a single tube natural circulation evaporator the coexistence of DWO of different orders at transition points. These are not stable and change arbitrarily. Chen et al. [9] studied experimentally the effect of power changing procedure on the thermohydraulic behaviour of a double channel natural circulation loop. They found a hysteresis effect at the onset of two-phase flow in which, depending on the power changing procedure, single-phase flow or an oscillating operational state arises.

An evaluation of literature shows that hysteresis effects on the field of two-phase flow and boiling heat transfer include flooding transition [25] or the onset of nucleate boiling [26]. However, experimental works, studying multiple states in natural circulation evaporators, are still extremely rare, as shown above.

In this contribution, the different operational states appearing in an open natural circulation evaporator at low subcoolings and heating steam pressures up to 0.44 MPa are presented. The rarely studied modes of geysering coupled with manometer oscillations and type I density wave oscillations first to third order and their transitions are analysed in detail. For the first time the coexistence of three modes with different driving mechanisms (geysering, DWO type I second and third order) at single parameter constellations is shown. By distinct disturbance of the system, the individual operational mode can be set.

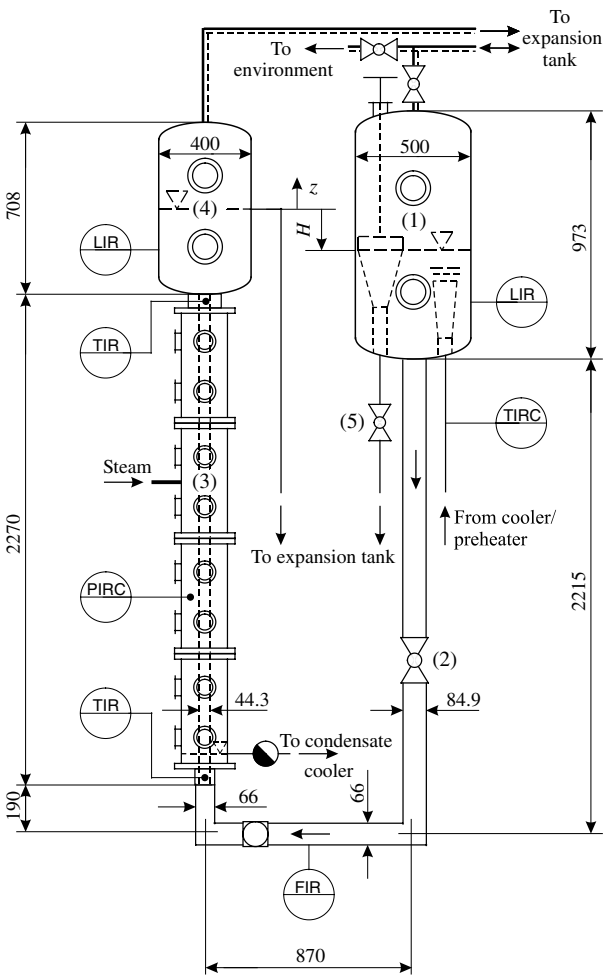

Fig. 1. Schematic illustration of the experimental set-up, (1) supply tank, (2) feeding line with ball valve, (3) steam heated evaporator, (4) steam separator (riser), (5) ball valve, units: mm.

2. Experiment

2.1. Apparatus

The test facility consists of a U-tube connected to a supply tank (1) and steam separator (4) at its open ends (see Fig. 1). One side of the U-tube is steam heated (3). To realise both, proper adjustable temperatures of the process medium and a low pressure drop in the feeding line of the heat exchanger, the supply tank and the steam separator are not connected to each other directly. Hence, liquid is conveyed from the expansion tank by a radial pump through a pipe in pipe cooler into the supply tank (1). The coolant flow rate of the heat exchanger is controlled; therefore, the liquid enters the supply tank with a defined temperature. One part of the liquid leaves this tank by an adjustable overfall back into the expansion tank in order to maintain a constant liquid level in the chamber. The remaining part enters the U-tube. In the steam separator (4), the liquid phase returns to the expansion tank by an overfall situated in the wall. The vapour leaves the separator by a second tube for the expansion tank, from where it disappears into the environment. The head spaces of all three tanks are connected to each other by tubes. Hence, a unique static pressure exists in all tanks at the liquid surfaces.

This apparatus constellation satisfies the condition for natural circulation mode if the liquid charging level H in the supply tank is greater than or equal to zero. Here, the coordinate H starts at the height of the overfall in the steam separator and grows with decreasing liquid level in the supply tank, Fig. 1. The pressure drop coefficient of the feeding line can be set by a ball valve (2). The steam heated tube in the evaporator with a heated length of 2 m and a wall thickness of 2 mm features an electro polished inner wall. The heating steam pressure is controlled. Before entering the shell side of the evaporator, a steam dryer separates the liquid from the vapour phase of the heating steam. After condensation, the liquid leaves the evaporator by a ball float trap and a condensate cooler to avoid evaporation as a result of pressure release. In all tanks, the evaporator and its feeding line feature inspection glasses for observation of two-phase flow pattern and the shape of liquid surfaces respectively. The tubes and tanks consist of stainless steel. Insulation of the apparatus with glass fibre minimises heat removal.

2.2. Data acquisition

Platinum thermometers (PT 100) in 4-wire technique in casing pipes (diameter 2 mm, wall thickness 0.2 mm) serve for temperature measurements at both the inlet and the outlet of the evaporator (TIR in Fig. 1). The sensors have been calibrated together with the transmitters. The volume flux in the U-tube (FIR) is determined by a magnetic inductive flowmeter (Endress and Hauser, Promag 33 H) and the height of liquid levels in the supply tank and steam separator (LIR) by differential pressure transmitter (Vega, Vegadif 34). A pressure transmitter by Haenni (ED 510) detects the pressure of heating steam (PIRC). The flow rate of the heating steam condensate is determined by a simple method of temperature and time measurement the liquid requires filling a defined volume. A PLC (programmable logic controller) by Texas Instruments (Typ 545) controls heating steam pressure, feeding temperature of the U-tube and flow rate of the liquid entering the supply tank. For data acquisition, a board by National Instruments (PCI-MIO-16E-4) and LabView is used in combination with a personal computer.

2.3. Experimental procedure/data analysis

The experiments start by heating up the system and setting the following parameters: temperature of liquid in the feeding line ϑ_F, heating steam pressure p, liquid charging level H in the supply tank, pressure drop coefficient ζ_I of feeding line and the flow rate through the cooler. All experiments have been carried out with water as the working fluid at ambient pressure. The parameters and the investigated range are listed in Table 1. The pressure drop coefficient is obtained experimentally and referred to the specific kinetic energy of the liquid at the inlet velocity of the heated channel.

After setting the parameters, the temporal progressions of flow rate and temperatures are observed. If no temporal change of the behaviour appears within eight minutes and if ϑ_F shows at most a maximum deviation of ± 0.5 K from the scheduled value, data are recorded every 0.1 s for 8 min. During each measurement, the experimenter observes the two-phase flow pattern in the steam separator leaving the evaporator. The repeatability of measurements is investigated by repetitions at selected parameter constellations carried out at different days. To investigate the stability of every operational mode, the system is disturbed by limited temporal changes of the height of liquid level in the feeding tank and the pressure drop coefficient in the feeding line. This is achieved by either, closing valve (5) or by closing valve (2) in Fig. 1, respectively.

Table 1
Parameter settings

Heating steam pressure, p	0.12–0.44 MPa
Temperature feeding liquid, ϑ_F	61; 71; 81; 86 °C
Liquid charging level, H	25; 50; 75; 100 mm
Pressure drop coefficient inlet heat exchanger, ζ_I	0.4–72
System pressure	Ambient pressure
Volume flux cooler	$4,8 \times 10^{-3}$ m^3/s
Working fluid	Deionised water

The periodic time of transient operational modes is calculated by applying fast Fourier transformation on the volume flux/time curve delivered by the magnetic inductive flowmeter in the feeding line. Due to the strong nonlinear behaviour of the system this method is only used to obtain the fundamental frequency.

3. Results

For convenience, the results are partly interpreted by using dimensionless numbers. This is not a complete set of numbers, but adequate to present the results more clearly. The time t and the periodic time T are normalized by L_H/v_c, where L_H represents the length of the heated tube and v_c the characteristic velocity $v_c = \sqrt{g(H + d/4)}$. The latter value is characteristic for the velocity, the liquid would flow from the steam separator to the feeding tank. The parameter H denotes the height of liquid in the feeding tank and d the diameter of the overfall in the steam separator. The term $d/4$ takes in consideration, that the maximum liquid level in the steam separator is always increased due to the operational behaviour of the overfall. The velocity at the inlet of the evaporator v_I is divided by the characteristic velocity v_c to obtain the normalized mass flux $\dot{m}^*$. Here, identical densities of the origin and referred mass flux are supposed. The subcooling at inlet (I) and exit (E) of the heat exchanger are referred to $(\vartheta_b - \vartheta_F)$, the temperature difference between boiling temperature at the exit of the heated tube and the temperature of the feeding liquid. If superheating is not taken into consideration, this represents the maximum appearing temperature difference within the process medium. In the following, the ratio N_{Bo}/N_{Sub} is used as a non-dimensional parameter. The boiling number N_{Bo} describes the ration of added heat flow $\dot{Q}$ to the process medium and the heat flow required for evaporating the process medium. The value $\dot{Q}$ is calculated from the condensate mass flow and corrected by the experimentally obtained rate of heat loss. The mass flow in the denominator is formed with the characteristic velocity v_c. In comparison to the boiling number, the subcooling number N_{Sub} contains in the numerator the heat flow required to shift the process medium from subcooled to saturated state.

Chiang et al. [27] apply a similar but dimensional value which they call modified heat flux. It contains the quotient heat flux to subcooling of the process medium in the feeding line of the evaporator. They plot the time averaged velocity at the inlet of the evaporator versus the modified heat flux for an oscillating operational state in a natural circulation evaporator. Here, a unique curve appears, independent from the inlet subcooling.

Fig. 2 shows the periodic time of the investigated operational states versus heating steam pressure for a tempera-

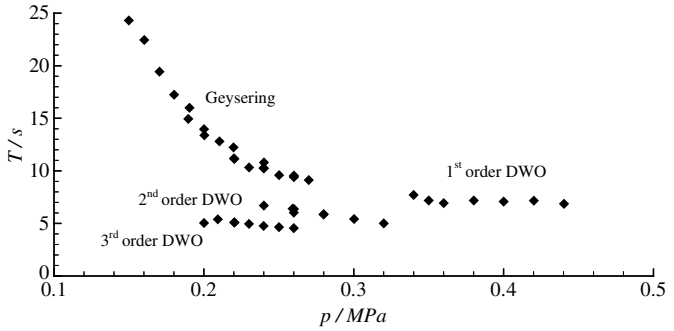

Fig. 2. Periodic time T versus heating steam pressure p for $\vartheta_F = 71$ °C, $H = 75$ mm and $\zeta_I = 0.4$.

ture of the feeding liquid $\vartheta_F = 71$ °C, a height of liquid level $H = 75$ mm and a pressure drop coefficient of $\zeta_I = 0.4$. Here, geysering and density wave oscillations (DWO), as well as the orders three, two and one of DWO, arise with increasing heating steam pressure/heat flux. At the transition between operational states, a discontinuity of the periodic time appears, as well as the coexistence of up to three modes (geysering coupled with manometer oscillations, second and third order DWO). Before describing the latter phenomenon in detail, the different operational states are introduced.

3.1. Geysering coupled with manometer oscillations

This mode is characterized by periodic, violent flow expulsions of a vapour/liquid mixture which lead to considerable vibrations of the experimental set-up. It shows the typical course of geysering: (a) incubation, (b) vapour generation/expulsion and (c) refilling (see Fig. 3). The diagrams depict the mass flux in the heat exchanger $\dot{m}^*$, the height of the liquid level in the steam separator z^* and the subcooling at inlet $\Delta\vartheta^*_{I\,Sub}$ and outlet $\Delta\vartheta^*_{E\,Sub}$ of the heat exchanger versus time τ for a typical sequence. All curves show almost constant amplitude.

During incubation, the liquid is partially heated up to a saturated/superheated state. The system becomes unstable. An arbitrary disturbance leads to a decrease of the static pressure in the heated tube and the generation of bigger amounts of vapour occurs (see also [19]). First, the vapour/liquid mixture is expelled to both sides of the heated tube. This can be recognized by the absolute minimum of the mass flux $\dot{m}^*$ and the local maximum of z^* at the beginning of vapour generation/expulsion. Following this, the two-phase flow is accelerated towards the steam separator by buoyancy force. The subcooled liquid from the feeding tank then refills the heated zone and displaces the gas phase completely, the sequence restarts.

Depending on the phase, this mode shows different two-phase flow pattern at the outlet of the heated tube. After onset of vapour generation first single liquid phase and then a few bubbles, pushed by slug bubbles appear at the outlet of the heated channel. Subsequent churn flow and bubbly flow follow before the single liquid phase appears again with cords during refilling. The cords result from an inhomogeneous density distribution of the liquid in the tank.

In comparison to pure geysering, this mode exhibits a superposed manometer oscillation. This will be explained in the following.

Experiments in the concerned U-tube under isothermal conditions with single-phase flow show a weakly damped manometer oscillation of the liquid water column with a periodic time

$$T_U = 2\pi\sqrt{L/g}, \tag{2}$$

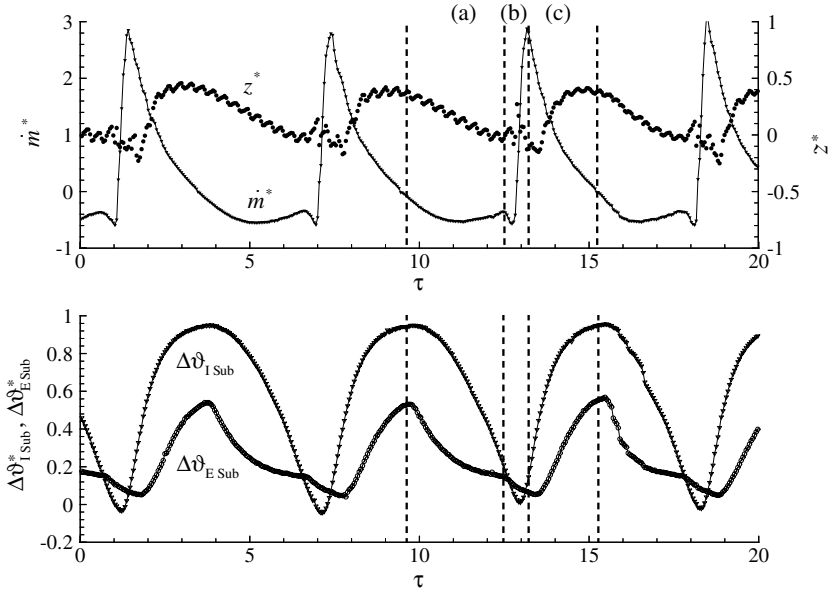

Fig. 3. Mass flux $\dot{m}^*$, liquid level in the steam separator z^*, subcooling at the inlet $\Delta\vartheta^*_{I\,Sub}$, and exit $\Delta\vartheta^*_{E\,Sub}$ of the heated tube versus time τ in dimensionless form for geysering ($\vartheta_F = 71$ °C, $p = 0.24$ MPa, $H = 75$ mm, $\zeta_I = 0.4$).

where

$$L = \sum_i \frac{A_S}{A_i} L_i.$$

Here, L_i and A_i represent the lengths and the cross sectional areas of all liquid filled tubes/tanks of the U-tube. The comparison of the analytical solution with measured values shows a maximum deviation of ±3.6%.

In the heated case, the manometer oscillation can be recognized easily during refilling and incubation. At the beginning of the refilling period, liquid flows from the feeding tank towards the steam separator while the liquid level in the steam separator is rising. A partial change from kinetic to potential energy takes place. The remaining part of energy leaves the U-tube system with the liquid at the overfall in the steam separator and/or is converted to internal energy of the fluid by friction. At the beginning of incubation, the liquid velocity in the U-tube is equal to zero and the liquid level in the steam separator is higher than in the feeding tank. Therefore, an acceleration of the liquid from steam separator to feeding tank and a partial change from potential energy to kinetic energy occurs. The onset of the geyser stops the conversion. Hence, this can be described as a forced oscillation – the periodically appearing geyser feeds kinetic energy to the system to maintain the damped manometer oscillation.

In the investigated parameter range, the periodic time of the isothermal manometer oscillations T_U is greater than that of the geyser T. Therefore, no complete period of the manometer oscillation arises (Fig. 3). The periodic time T decreases with rising heating steam pressure. This results from the increased heat flow and leads to shorter incubation periods. Geysering also exists without manometer oscillations [17]. In the case of pure geysering, the liquid remains almost static in the heated channel during incubation. Hence, the heat transfer is dominated by conduction in this phase. With manometer oscillation, transient flow and therefore convective heat transfer arises in the evaporator for time periods:

(1) $T > T_U$ with alternating flow direction, observed by [20] and for
(2) $T < T_U$ with uniform negative flow direction, presented in this work.

During incubation, liquid in riser ($T > T_U$) and feeding line ($T > T_U$, $T < T_U$) is heated up in addition to liquid in the heated channel. The residence time distribution of liquid in the heated channel leads to altered radial but especially axial temperature profiles in the U-tube in comparison to the static case. This influences time and intensity of the succeeding geyser: As result of the backflow during incubation, the liquid is heated up from outlet to inlet of the heated tube. The negative values of the subcooling at the entry of the heated tube indicate that superheated liquid (with respect to ambient pressure) is stored in the feeding line. The volume of preheated liquid in the feeding line can exceed one to the twofold of the heated tube. During vapour generation and expulsion, the pressure in the liquid decreases due to change of geodetic height, density and acceleration of the fluid. The superheated liquid in the feeding line contributes to an additional generation of vapour volume. This leads to an increased intensity of the geyser in comparison to pure geysering. Due to flashing, the maximum mass fluxes, 20–60 times higher than the time averaged value, can be observed.

The geometry of the experimental set-up influences strongly its operational behaviour. Therefore, the appearance of geysering with manometer oscillation has been rarely mentioned in literature. In comparison to plants described in literature [15,17,22,28], this facility features extreme low pressure drop coefficients of the feeding line ($\zeta_I = 0.4$) and an extremely high ratio of cross sectional area steam separator to heated tube ($A_S/A_H = 81$). This enables the appearance of weakly damped manometer oscillations with time periods greater than that of geysering.

3.2. Density wave oscillations type I

Fig. 4 depicts typical curves of mass flux and subcooling at the exit of the heated channel versus time for DWO type I, first, second and third order.

All curves are characterized by a periodic, sinusoidal behaviour with almost constant amplitudes, similar to velocity measurements by Saha et al. [29]. In comparison to geysering, this mode shows a less violent behaviour with much smaller amplitudes of mass fluxes and subcoolings. The flow pattern at the outlet of the heated tube exhibit bubbly and partially slug flow. The mechanism of density wave oscillations is sufficiently described in literature, see [12] for a review, and therefore not mentioned here. The classification of the observed operational states to DWO type I of different orders is based upon two characteristics:

(1) Thermodynamic state of the fluid at the outlet of the evaporator.
(2) Relation between time period of oscillation and transit time of an enthalpy perturbation in the liquid filled part of the heated channel.

Measurements of temperature at the outlet of the evaporator reveal for first and second order DWO, a time averaged subcooled fluid (Fig. 4). Hence, these operational states are characterized by a low steam quality in the evaporator. Furthermore, the time averaged mass flux of all orders increases with rising difference between heating steam temperature and boiling temperature ($\vartheta_{HS} - \vartheta_b$) respectively with growing N_{Bo}/N_{Sub} (Fig. 5).

The non-dimensional numbers vary in the range of one, which confirms that the characteristic values are of relevant order of magnitude. The data points show a nearly linear behaviour with N_{Bo}/N_{Sub}. The extrapolation of $N_{Bo+}/N_{Sub} \to 0$ leads to the physically correct result $\dot{m}^* \to 0$.

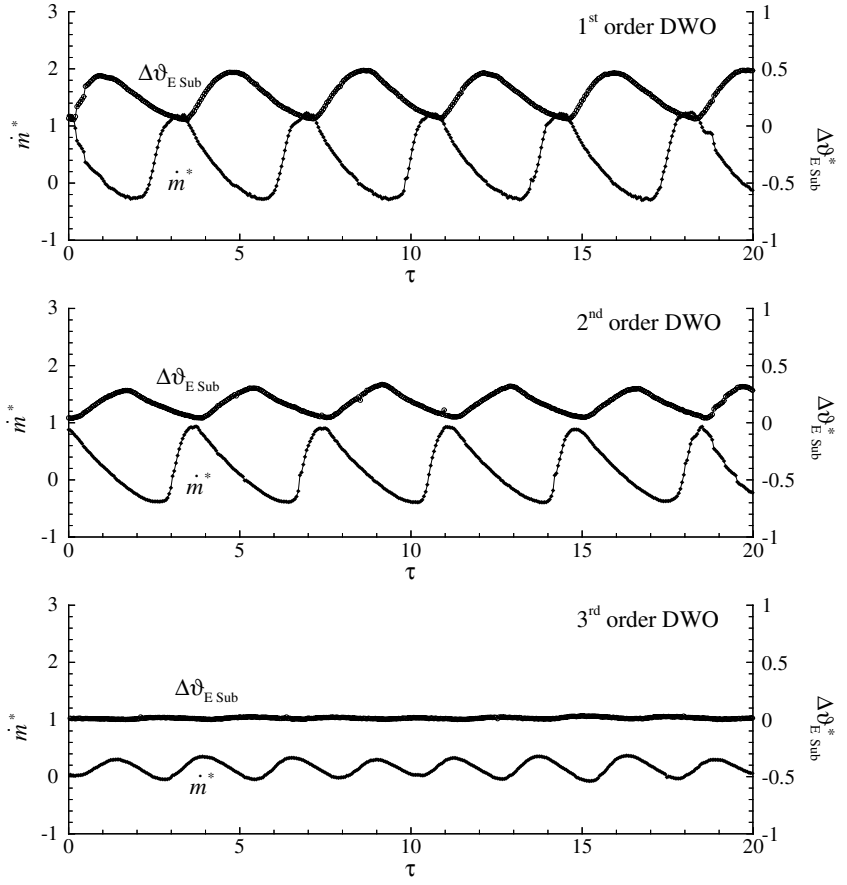

Fig. 4. Mass flux $\dot{m}^*$, and subcooling at the exit $\Delta\vartheta^*_{E\,Sub}$ of the heated section versus time τ in dimensionless form for density wave oscillation first order ($\vartheta_F = 71$ °C, $p = 0.40$ MPa, $H = 75$ mm, $\zeta_I = 0.4$), second order ($\vartheta_F = 71$ °C, $p = 0.24$ MPa, $H = 75$ mm, $\zeta_I = 0.4$) and third order ($\vartheta_F = 71$ °C, $p = 0.24$ MPa, $H = 75$ mm, $\zeta_I = 0.4$).

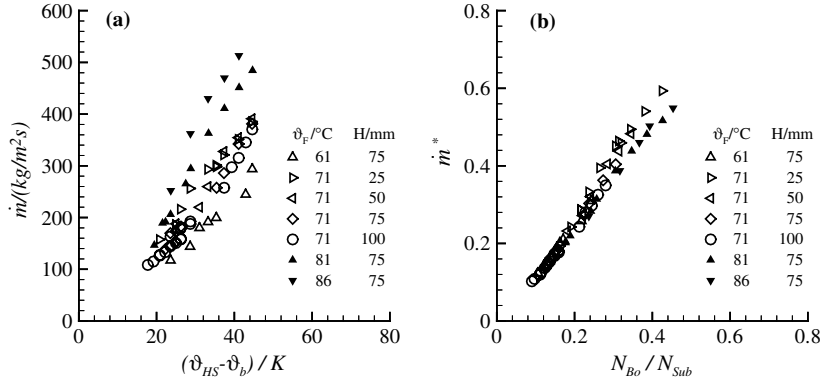

Fig. 5. Time averaged mass flux versus difference between heating steam temperature and boiling temperature ($\vartheta_{HS} - \vartheta_b$) and N_{Bo}/N_{Sub} for first to third order DWO.

The course of mass flux versus N_{Bo}/N_{Sub} and ($\vartheta_{HS} - \vartheta_b$) indicates that phase change induced gravitational pressure drop governs the flow behaviour in the evaporator. Fukuda and Kobori [22] recognize this as a characteristic of DWO type I.

The fulfilment of the second characteristic can be shown by applying the relation by Yadigaroglu and Bergles [23] to the experimental data (Eq. (1)). The value n describes the number of periodic times a fluid element needs to pass the liquid filled length z_{bb} of the heated channel. To receive z_{bb}, thermodynamic equilibrium of the fluid and a constant heat flux along the heated channel are assumed. The application of energy equation leads to

$$z_{bb} = L_H \frac{v_I A_H \rho_F c_p (\vartheta_b - \vartheta_F)}{\dot{Q}}, \tag{3}$$

where A_H describes the cross sectional area, L_H the length of the heated tube, ρ_F the density, T_F the temperature of the feeding liquid, $\dot{Q}$ the heat flow and ϑ_b the boiling temperature. The wave length of the enthalpy oscillations is obtained from

$$\lambda = v_I T, \tag{4}$$

where v_I represents the time averaged velocity of the liquid at the inlet of the heat exchanger, and T the periodic time of the density wave oscillation. By insertion of Eqs. (3) and (4) in (1), the order

$$n = \frac{L_H A_H \rho_F c_p (\vartheta_b - \vartheta_F)}{T\dot{Q}} \tag{5}$$

can be calculated. Fig. 6 presents the results versus N_{Bo}/N_{Sub}.

Obviously, the data points in the diagram group around the values $n = 1$, 2 and 3. Hence, for the first time, this work clearly shows the existence of higher mode DWO of type I. The marked areas around the orders show the variation range of n due to measurement uncertainties. Deviations from these ranges result from effects occurring at the transition of modes, as well as from the simplified assumptions stated above. The data point at $n = 4$ suggests the existence of a fourth order. However, this could not be confirmed by further measurements at lower values for N_{Bo}/N_{Sub}.

The transformation of Eq. (5) combined with the definition of N_{Bo}/N_{Sub} provides a dimensionless relation for the periodic time

$$T^* = \frac{1}{n}\frac{N_{Sub}}{N_{Bo}}. \tag{6}$$

This equation clarifies, that the periodic time behaves reciprocally proportional to N_{Bo}/N_{Sub} and order n. The good agreement between calculated and experimental data for the periodic time of DWO is shown in Fig. 7.

The relation has no validity for geysering because of the completely different driving mechanism. Furthermore, Fig. 7 clarifies that the different modes appear within distinct ranges of N_{Bo}/N_{Sub}. At the transition range, they differ clearly in values of periodic time. In regard to the change from third to second order DWO, a discrete step

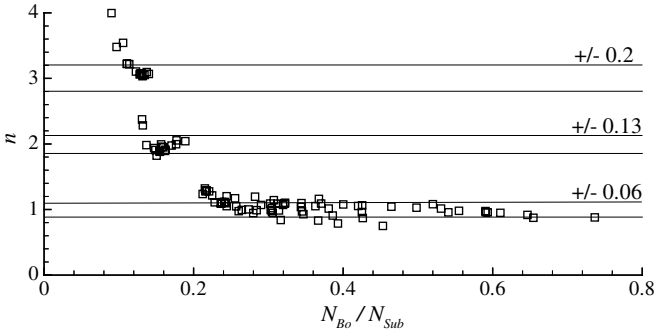

Fig. 6. Order n versus N_{Bo}/N_{Sub} for $\zeta_I = 0.4$.

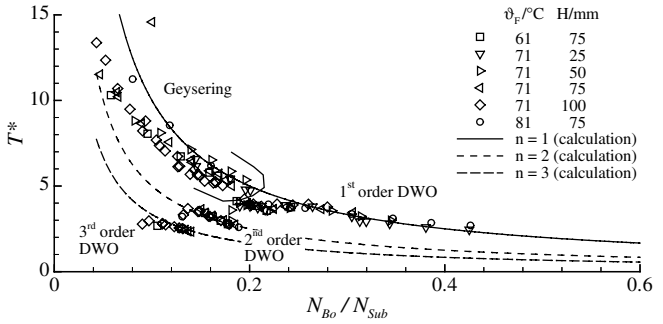

Fig. 7. Calculated and experimental data of periodic time T^* versus N_{Bo}/N_{Sub} for different temperatures of the feeding liquid ϑ_F, different liquid charging levels H, and $\zeta_I = 0.4$.

of T can be recognized in accordance with observations by [23]. They explain this behaviour with the interaction between enthalpy nodes in the single-phase region of the channel and the boiling boundary. With increasing heat flow and N_{Bo}/N_{Sub}, the enthalpy nodes move in the direction of the channel outlet. If a node reaches the boiling boundary, the order of the operational state is reduced and the periodic time increased.

The change from second to first order DWO is characterized by a more smooth transition (Fig. 7). The behaviour of the mass flux versus time of a transitional mode confirms this impression (Fig. 8).

The sequence contains wave trains with periodic times of both, first and second order DWO. The two different oscillations seem to appear successively with time. The results of a FFT analysis confirm this observation. Fig. 9 depicts five spectra which show the impact of growing N_{Bo}/N_{Sub} on the periodic time.

The first spectrum shows a pure second order oscillation and the last spectrum a pure first order oscillation. Here, the peaks of the dominating periodic time can be recognized easily and the spectra are similar. Between second and first order oscillations, both characteristic peaks exist. With rising N_{Bo}/N_{Sub}, the second order peak gradually decreases in comparison to the first order peak. In this parameter range, not one of the two described modes is stable. Slight disturbances, which appear continuously in two-phase flow [11], lead to a more or less arbitrary change of the mode. With increasing N_{Bo}/N_{Sub}, all spectra move

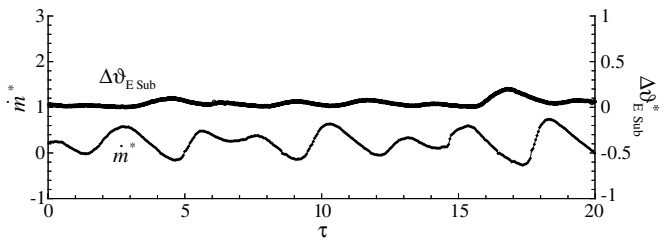

Fig. 8. Mass flux $\dot{m}^*$, and subcooling $\Delta\vartheta^*_{E\,Sub}$ at the exit of the heated section versus time τ for transition of DWO between first and second order ($\vartheta_F = 71$ °C, $p = 0.32$ MPa, $H = 75$ mm, $\zeta_I = 0.4$).

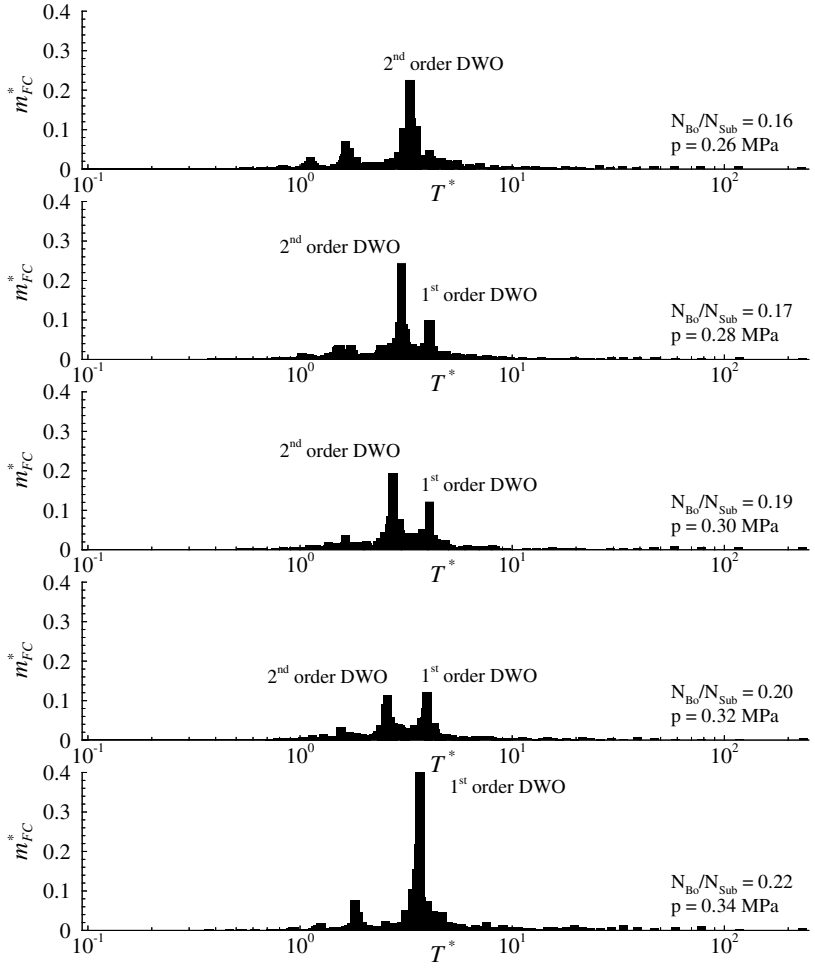

Fig. 9. Spectra of FFT analysis from the mass flux ($\vartheta_F = 71$ °C, $H = 75$ mm, $\zeta_I = 0.4$).

towards lower periodic times. The latter phenomenon arises also in the case of a single mode as described for geysering.

3.3. Multiple operational states at one parameter constellation

As mentioned above, at the transition from geysering to density wave oscillation, there exists a small parameter range where up to three operational states occur – geysering, second and third order DWO (Fig. 2). To set the different modes, two procedures have been investigated,

(1) defined change of a boundary condition and
(2) short-time perturbation of the system.

In the first case, the heating steam pressure/temperature of the evaporator follows a certain course. Starting with geysering at lower heating steam pressures p, an increase in p results in the succession of modes, denoted by hollow arrows in Fig. 10. Choosing second order DWO as the initial condition, the decrease of heating steam pressure leads to a transition to geysering at a lower value for p in comparison to the first course (filled arrows). This is the typical behaviour of a hysteresis also found by Chen et al. [9] for the modes of steady single-phase flow and transient two-phase flow oscillation. By this procedure, the mode third order DWO does not appear.

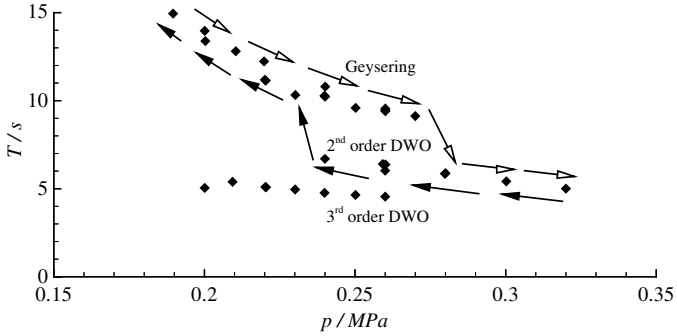

Fig. 10. Periodic time T versus heating steam pressure p for $\vartheta_F = 71$ °C, $H = 75$ mm, and $\zeta_I = 0.4$.

A second possibility to change between operational states consists of temporary limited perturbations of the system. This is realized by (a) short-time increase of the

pressure drop coefficient ζ_I in the feeding line or (b) short-time rise in liquid charging level H in the feeding tank. For this, two ball valves (see (2) and (5) in Fig. 1) are available. The first one serves for throttling, the second one to heighten the liquid level in the feeding tank.

Starting with geysering at a parameter constellation where all three operational states can occur, a temporary increase in the pressure drop coefficient leads to second and third order DWO (Fig. 11). In this diagram the amplitude of the mass flux is plotted versus the pressure drop coefficient ζ_I. The transition of modes takes place at a critical value of ζ_I. By putting the pressure drop coefficient back to the initial value, the current mode remains. The period of perturbation can range from a few seconds to several minutes to set the new operational state.

The rise in liquid charging level H in the feeding tank acts conversely to throttling. Depending on the height, a transition to a mode of higher periodic time can be observed. A sequence of changes of modes after short-time perturbations is displayed in Fig. 12. Here, the mass flux in the U-tube and the height of liquid level H in the feeding tank are plotted versus time. Beginning with third order DWO as the initial state, a temporal limited rise in H provokes the transition to second order DWO and a further increase to geysering. The initial state is restored by short-time throttling.

The change in operational states by perturbation can be explained by the impact of the specific perturbation in combination with the mechanism of the mode. The transition from geysering to second order DWO due to short-time throttling results from the change of kinetic to internal energy. The influence of the increased value of ζ_I can be recognized especially during vapour generation and expulsion. In this phase, the highest flow velocities and kinetic energies of the fluid appear. Throttling interrupts the cycle of periodic conversion from kinetic to potential energy by change of kinetic energy to internal energy. The lack of potential energy at the beginning of incubation prevents backflow in the heat exchanger. This leads to higher residence times of liquid elements in the heated tube. Furthermore, almost no preheated liquid is stored in the feeding line. Hence, vapour generation starts earlier but less intensive. The kinetic energy during vapour generation is not sufficient to fan geysering. The mode then changes to second order DWO.

In the case of DWO, an increase in the pressure drop coefficient leads to reduced time averaged mass fluxes in the system, and therefore to a displacement of the enthalpy nodes in the liquid filled part of the heated tube towards the entry. During a sufficiently high decrease in mass flux, a new node is formed at the boiling boundary, which results in a change from second to third order DWO.

The rise in liquid level in the feeding tank acts conversely to throttling, whereby enthalpy nodes move towards the boiling boundary (transition third to second order DWO) respectively potential energy is fed into the system (transition second order DWO – geysering). Starting with third order DWO, a change to second order DWO or geysering takes place depending on the perturbation of the liquid charging level in the feeding tank.

With the knowledge of the effect of temporary perturbations on the system, it is possible to carry out defined changes between the operational states, presented in Fig. 12.

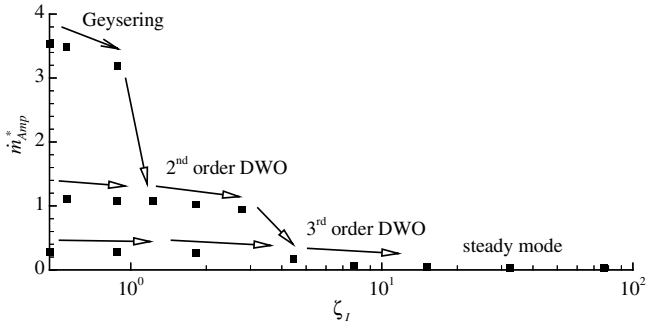

Fig. 11. Amplitude of mass flow $\dot{m}^*_{Amp}$ versus pressure drop coefficient ζ_I ($p = 0.25$ MPa, $\vartheta_F = 71$ °C, $H = 75$ mm).

4. Conclusion

The operational behaviour of an open single tube, steam heated, natural circulation evaporator has been investigated. At subcoolings of 14–39 K and heating steam pressures of 0.12–0.44 MPa, different operational modes appear. With rising heating steam pressure and decreasing subcooling, geysering coupled with manometer oscilla-

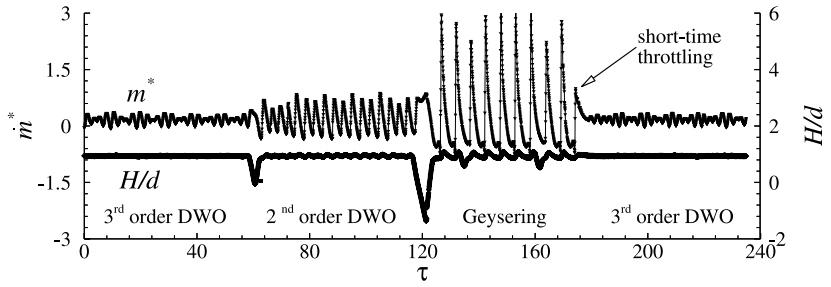

Fig. 12. Defined change between second, third order DWO, and geysering by short-time perturbation of the system ($p = 0.25$ MPa, $\vartheta_F = 71$ °C, $H = 75$ mm, $\zeta_I = 0.4$).

tions, third order, second order and first order of density wave oscillations type I arise. All modes show a periodic behaviour and have been rarely described in literature up to now. The first operational state shows the typical sequence of geysering: (a) incubation, (b) vapour generation/expulsion and (c) refilling. Due to the superposed manometer oscillations, backflow occurs in the heated tube during incubation. Hence, saturated liquid is stored in the feeding line. During vapour generation, the stored liquid intensifies the geyser by flashing which leads to considerable vibrations of the plant. The remaining modes show a strong correlation between periodic time of the oscillation and travelling time of enthalpy perturbations in the liquid phase of the heated tube. Furthermore, low vapour quality could be observed at the exit of the heat exchanger, which are characteristics of type I density wave oscillations.

By calculating the order of the DWO (ratio between length of single-phase region and wavelength of the enthalpy oscillations in the single-phase region) from experimental data, the oscillations can be divided into first, second and third order. The periodic time of DWO behaves proportionally to subcooling number and reciprocally proportional to boiling number and order.

Due to the strong nonlinear behaviour of natural circulation evaporators, up to three modes (geysering coupled with manometer oscillations, second and third order DWO) appear at one parameter constellation. By adopting a defined setting of the boundary conditions or short-time perturbation of the system, the different modes can be set.

References

[1] K. Hibi, H. Ono, T. Kanagawa, Integrated modular water reactor (IMR) design, Nucl. Eng. Des. 230 (2004) 153–266.

[2] A.K. Nayak, P.K. Vijayan, D. Saha, V. Venkat Raj, M. Aritomi, Study on the stability behaviour of a natural circulation pressure tube type boiling water reactor, Nucl. Eng. Des. 215 (2002) 127–137.

[3] J.H. Hills, W.E. Jones, A.K. Ibrahim, The behaviour of a pilot-scale horizontal thermosyphon reboiler, Trans. IChemE, Part A 75 (1997) 652–656.

[4] A.W. Sloley, Properly design thermosyphon reboilers, Chem. Eng. Progr. 3 (1997) 52–64.

[5] A. Baars, F. Werner, A. Delgado, Investigations on the maximum inner wall temperature in a steam heated tube with natural circulation for the use in biotechnology, in: B.J. Grochal, J. Mikielewicz, B. Sunden (Eds.), Proceedings of the Third Baltic Heat Transfer Conference, IFFM Publishers, Gdansk, 1999, pp. 509–514.

[6] N. Abe, S. Yokobori, H. Nagasaka, S. Tsunoyama, Two-phase flow natural circulation characteristics inside BWR vessels, Nucl. Eng. Des. 146 (1994) 253–265.

[7] D. Brück, Einfluss mechanischer Belastungen auf dispergierte, empfindliche Inhaltsstoffe von Flüssigkeiten in Leitungssystemen und Behälterströmungen, PhD thesis, Technische Universität München, 1997.

[8] C. Schuster, A. Ellinger, J. Knorr, Analysis of flow instabilities at the natural circulation loop DANTON with regard to non-linear effects, Heat Mass Transfer 36 (2000) 557–565.

[9] W.L. Chen, S.B. Wang, S.S. Twu, C.R. Chung, C. Pan, Hysteresis effect in a double channel natural circulation loop, Int. J. Multiphase Flow 27 (2001) 171–187.

[10] J.M. Kim, S.Y. Lee, Experimental observation of flow instability in a semi-closed two-phase natural circulation loop, Nucl. Eng. Des. 196 (2000) 359–367.

[11] J.A. Bouré, A.E. Bergles, L.S. Tong, Review of two-phase flow instability, Nucl. Eng. Des. 25 (1973) 165–192.

[12] G. Yadigaroglu, Two-phase flow instabilities and propagation phenomena, in: J.M. Delhaye, M. Giot, M.L. Riethmuller (Eds.), Thermohydraulics of Two-phase Systems for Industrial Design and Nuclear Engineering, McGraw-Hill, New York, 1981, pp. 353–403.

[13] G. Yun, G.H. Su, J.Q. Wang, W.X. Tian, S.Z. Qiu, D.N. Jia, J.W. Zhang, Two-phase instability analysis in natural circulation loops of China advanced research reactor, Ann. Nucl. Energy 32 (2005) 379–397.

[14] A. Manera, T.H.J.J. van der Hagen, Stability of natural-circulation-cooled boiling water reactors during startup: experimental results, Nucl. Technol. 143 (2003) 77–88.

[15] M.H. Subki, M. Aritomi, N. Watanabe, H. Kikura, T. Iwamura, Transport mechanism of thermohydraulic instability in natural circulation boiling water reactors during startup, J. Nucl. Sci. Technol. 40 (2003) 918–931.

[16] S.Y. Jiang, Y.J. Zhang, X.X. Wu, J.H. Bo, H.J. Jia, Flow excursion phenomenon and its mechanism in natural circulation, Nucl. Eng. Des. 202 (2000) 17–26.

[17] I.K. Kyung, S.Y. Lee, Experimental observations on flow characteristics in an open two-phase natural circulation loop, Nucl. Eng. Des. 159 (1994) 163–176.

[18] S.Y. Jiang, M.S. Yao, J.H. Bo, S.R. Wu, Experimental simulation study on start-up of the 5 MW nuclear heating reactor, Nucl. Eng. Des. 158 (1995) 111–123.

[19] P. Griffith, Geysering in liquid-filled lines, ASME Paper 62-HT-39, 1962.

[20] B.A. Hands, The flow stability of a liquid-nitrogen thermosyphon with 8 mm bore riser, AIChE Symp. Ser. No. 189, vol. 75, 1979, pp. 177–184.

[21] M. Aritomi, J.H. Chiang, T. Nakahashi, M. Wataru, M. Mori, Fundamental study on thermo-hydraulics during start-up in natural circulation boiling water reactors (I), Nucl. Sci. Technol. 29 (1992) 631–641.

[22] K. Fukuda, T. Kobori, Two-phase flow instability in parallel channels, in: Sixth International Heat Transfer Conference, 1978, FB-17, pp. 369–374.

[23] G. Yadigaroglu, A.E. Bergles, Fundamental and higher-mode density-wave oscillations in two-phase flow, J. Heat Transfer Trans. ASME 94 (1972) 189–195.

[24] A. Knaani, Y. Zvirin, Bifurcation phenomena in two-phase natural circulation, Int. J. Multiphase Flow 19 (1993) 1129–1151.

[25] S.G. Bankoff, S.C. Lee, Flooding and hysteresis effects in nearly horizontal countercurrent stratified steam-water flow, Int. J. Heat Mass Transfer 30 (1987) 581–588.

[26] H. Bräuer, F. Mayinger, Onset of nucleate boiling and hysteresis effects under forced convection and pool boiling, in: Proceedings of the Engineering Foundation Conference on Pool and External Boiling, Santa Barbara, 1992, pp. 15–36.

[27] J.H. Chiang, M. Aritomi, M. Mori, Fundamental study on thermo-hydraulics during start-up in natural circulation boiling water reactors (II), J. Nucl. Sci. Technol. 30 (1993) 203–211.

[28] V.K. Chexal, A.E. Bergles, Two-phase instabilities in a low pressure natural circulation loop, AIChE Symp. Ser. 131 (1973) 37–54.

[29] P. Saha, M. Ishii, N. Zuber, An experimental investigation of the thermally induced flow oscillations in two-phase systems, J. Heat Transfer, Trans. ASME 98 (1976) 616–622.